

1 Naturally Produced Lovastatin Modifies the Histology and Proteome Profile of
2 Goat Skeletal Muscle

3

4 Short title: Naturally produced lovastatin on histology and proteome profile

5

6 Teik Kee Leo¹, Sani Garba¹, Danmaigoro Abubakar², Awis Qurni Sazili^{1,3}, Su
7 Chui Len Candyrine⁴, Mohammad Faseleh Jahromi⁵, Yong Meng Goh^{1,2}, Ron
8 Ronimus⁶, Stefan Muetzel⁶, Juan Boo Liang^{1*}

9

10 ¹Institute of Tropical Agriculture and Food Security, Universiti Putra Malaysia,
11 Serdang, Selangor, Malaysia

12 ²Faculty of Veterinary Medicine, Universiti Putra Malaysia, Serdang, Selangor,
13 Malaysia

14 ³Faculty of Agriculture, Universiti Putra Malaysia, Serdang, Selangor, Malaysia

15 ⁴Faculty of Sustainable Agriculture, Universiti Malaysia Sabah, Sandakan,
16 Sabah, Malaysia

17 ⁵Agricultural Biotechnology Research Institute of Iran, Mashad, Iran

18 ⁶Rumen Microbiology, AgResearch, Palmerston North, New Zealand

19

20 *Corresponding author

21 E-mail: jbliang@upm.edu.my (JBL)

23 **Abstract**

24 Enteric methane formation in ruminants is one of the major contributors to
25 climate change. We have reported that supplementation of naturally produced
26 lovastatin reduced methane emissions in goats without adversely affecting
27 rumen fermentation and animal performance, except that at higher level,
28 lovastatin can have a negative effect on the palatability of the formulated diet.
29 As statins are associated with the development of muscle-related adverse
30 effects at higher than recommended therapeutic doses, this study was
31 conducted to examine the effects of lovastatin on the histology and proteome
32 profile of goat skeletal muscle. A total of 20 intact male Saanen goats were
33 randomly assigned in equal numbers to 4 groups, and fed with a total mixed
34 ration containing 50% rice straw, 22.8% concentrates and 27.2% of various
35 proportions of untreated or treated palm kernel cake (PKC) to achieve the target
36 daily intake levels of 0 (Control), 2 (Low), 4 (Medium) or 6 (High) mg
37 lovastatin/kg body weight (BW). Histological examination discovered that the
38 longissimus thoracis et lumborum muscle of animals from the Medium and High
39 treatment groups showed abnormalities in terms of necrosis, degeneration,
40 interstitial space and vacuolation. Western blot analysis conducted on the
41 myosin heavy chain showed that the immunoreactivity of myosin heavy chain in
42 the High treatment group was significantly lower than the Control, Low and
43 Medium treatment groups. Comparisons between control and lovastatin-treated
44 groups demonstrated that lovastatin supplementation induced complex
45 modifications to the protein expression patterns of the longissimus thoracis et
46 lumborum muscle of the goat. There were 30, 26 and 24 proteins differentially
47 expressed in Low, Medium and High treatment groups respectively, when

48 compared to the Control group. Supplementation of lovastatin down-regulated
49 proteins involved in carbohydrate and creatine metabolism, indicative of
50 reduced energy production, and may have contributed to the skeletal muscle
51 damage. Supplementation of naturally produced lovastatin induced muscle
52 damage in longissimus thoracis et lumborum muscle of goats with increasing
53 dosages, particularly at 6mg/kg BW. In addition, proteomics analysis revealed
54 that lovastatin supplementation induced complex modifications to the protein
55 expressions of skeletal muscle of goats which may have contributed to the
56 observed skeletal muscle damage. Present study suggested that
57 supplementation of naturally-produced lovastatin at 6mg/kg BW could adversely
58 affecting health and wellbeing of the animals.

59

60 **Introduction**

61 Methane gas is one of the major greenhouse gases that is contributing to
62 climate change. Livestock production has been reported to contribute
63 approximately 18% of methane emissions and 9% of carbon dioxide production
64 [1], which results primarily from the enteric fermentation of feeds [2]. Enteric
65 methane formation results from the activity of complex interactions of anaerobic
66 bacteria which together enable degradation of ruminant feeds and
67 methanogenic archaea which help remove metabolic hydrogen in the rumen [3].
68 Despite the importance of methanogenesis in maintaining low partial pressure
69 of hydrogen required for efficient ruminal fermentation, the formation of
70 methane also represents 2-12% loss of gross dietary energy [4]. Hence,
71 extensive research efforts are focused on the development of strategies to

72 modify ruminal fermentation for reduction of methane emissions [5] as well as
73 better feed utilization [6].

74

75 Among the potential strategies for mitigating methane emissions,
76 supplementation of feed additives such as ionophores [7], organic acids [8],
77 fatty acids [9], methyl coenzyme M reductase inhibitors [10], vaccine [11] and
78 oils [12] have been extensively researched. However, many of these strategies
79 have limited application due to their negative effect(s) on human and animal
80 health, animal performance parameters and economical acceptance [13].
81 Supplementation of naturally produced lovastatin is a promising approach for
82 mitigating methane emissions.

83

84 Lovastatin (C₂₄H₃₆O₅, M.W. 404.55) is a secondary product during the
85 secondary phase (idiophase) of fungal growth. It is a competitive inhibitor of 3-
86 hydroxy-3-methylglutaryl coenzyme A (HMG-CoA) reductase, which is a key
87 enzyme in the cholesterol production pathway [14]. Inhibition of HMG-CoA
88 reductase will mediate the suppression of cholesterol synthesis and cell
89 membrane formation in methanogenic Archaea. A previous study has shown
90 that significant reduction in growth and activity of methanogenic Archaea using
91 lovastatin without any negative effect on cellulolytic bacteria [15]. In addition,
92 naturally produced lovastatin has been shown to mitigate methane gas
93 emissions, while simultaneously enhancing digestibility of feed [16].

94

95 A previous study has reported the effects of naturally produced lovastatin from
96 fermented-*Monascus purpureus* red rice powder on cattle [17]. High dose of

97 fermented-*Monascus purpureus* red rice powder (100g/day and above)
98 supplementation adversely affected dry matter intake and ruminant physiology.
99 We have recently reported that supplementation of naturally produced lovastatin
100 in goats as being capable of mitigating methane emissions effectively without
101 adversely affecting digestion and rumen fermentation, except that animals fed
102 the highest level (6 mg/kg BW) had lower appetite [18]. Statins have been
103 associated with the development of muscle-related adverse effects, however
104 the effects of lovastatin on the skeletal muscle in goats have not been studied.
105 Therefore, this follow-up study was conducted to examine the effects of
106 lovastatin on the histology and proteome profile of the goat skeletal muscle from
107 the above study to further elucidate whether supplementation of lovastatin
108 affects the health and wellbeing of the goats.

109

110 **Material and Methods**

111 **Animals and management**

112 This study was approved by the Animal Care and Ethics Committee of the
113 Universiti Putra Malaysia (UPM/IACUC/AUP-R0087/2015). Detail protocols of
114 the study have been reported [18]. Briefly, twenty intact male Saanen goats of 4-
115 5 months old with average live weight of 26 ± 3.4 kg were used in the 12-week
116 feeding trial. The animals were randomly assigned in equal numbers and fed a
117 total mixed ration containing 50% rice straw, 22.8% concentrates and 27.2% of
118 various proportions of untreated or treated PKC to achieve the target daily
119 intake level of 0 (Control), 2 (Low), 4 (Medium) or 6 (High) mg lovastatin/kg BW.

120 The lovastatin was produced by solid state fermentation using PKC (palm
121 kernel cake) and *Aspergillus terreus* (ATCC 74135) [18].

122

123 **Slaughtering and sample collection**

124 At the end of feeding trial, the animals were humanely slaughtered according to
125 the standard protocol of halal (Muslim) slaughtering (MS1500:2009).
126 Immediately after skin removal and evisceration, longissimus thoracis et
127 lumborum muscle was collected from each animal. The muscle samples
128 collected for histology analysis were rinsed with normal saline solution before
129 fixing in 10% PBS buffered formalin solution. Muscle samples were snapped
130 frozen with liquid nitrogen for proteomics analysis and kept in -80°C until further
131 analysis.

132

133 **Histology**

134 Muscle samples were removed from the formalin solution, dehydrated in an
135 increasing ethanol series and routinely processed for paraffin embedding. The
136 samples were sectioned at 5 μm and stained with haematoxylin-eosin. From
137 each muscle, five locations were sectioned and each location was mounted on
138 a slide. and viewed with a Leica DM LB2 upright light microscope (Leica
139 microsystems Wetzlar GmbH, Wetzlar, Germany). Three images were captured
140 from each slide under 20 × magnification using a Leica DFC320 digital camera
141 connected to a computer which was controlled with Leica IM50 v4.0 software
142 (Leica microsystems Wetzlar GmbH, Wetzlar, Germany).

143

144 The muscle tissues were evaluated for evidence of necrosis, degeneration,
145 interstitial space and vacuolization. Numerical scores were assigned based on
146 degree of severity (0 = normal to 5 = severe) according to Gall et al. [19] (Table
147 1). Histological scores between every treatment groups were compared using
148 Kruskal-Wallis test. Statistical confidence was considered as $P < 0.05$.

149

150 **Table 1. Scoring system used in histological analysis on *longissimus***
151 ***thoracis et lumborum* muscle of goats supplemented with naturally**
152 **produced lovastatin.**

Score	Histopathologic injury	Percentage
0	Normal	0%
1	Minimal	<15%
2	Mild	≤25%
3	Moderate	≤ 40%
4	Marked	≥50

153

154 **Immunoblot analysis of myofibrillar proteins**

155 All muscle samples were pulverized into powder form with pestle and mortar
156 using liquid nitrogen. Myofibrillar proteins were extracted according to Morzel et
157 al. [20] with slight modifications. Approximately 100mg of muscle powder was
158 mixed with 1ml of extraction buffer containing 150mM NaCl, 25mM KCl, 3mM
159 MgCl₂, 4mM EDTA and 5μl of protease inhibitor (Calbiochem®) at pH6.5. The
160 mixture was vortexed for 30s before centrifuging at 500rpm for 5 min. After that,
161 the supernatant was transferred to a new tube, and centrifuged again at 4340
162 rpm for 15 mins at 4°C. The resulting pellet was washed twice with 1ml of

163 50mM KCl solution at pH6.4 and once with 1ml of 20mM phosphate buffer at
164 pH6. The pellet was eventually suspended in Tris-SDS buffer.

165

166 The extracted myofibrillar proteins were separated by sodium dodecyl sulphate-
167 polyacrylamide gel electrophoresis (SDS-PAGE) [21]. The proteins were mixed
168 with sample loading buffer (62.5mM Tris-HCl at pH6.8, 25% glycerol, 2% SDS,
169 0.01% (w/v) bromophenol blue and 5% β -mercaptoethanol) at ratio of 1: 5 and
170 incubated at 94°C for 5 min. For myosin heavy chain, the proteins were
171 separated with 4% stacking and 5% resolving gels. Whilst, other proteins were
172 separated with 4% stacking and 12% resolving gels for troponin T. The SDS-
173 PAGE was conducted at a constant current of 15mA/gel for 15 min, followed by
174 20mA/gel until the bromophenol blue dye reached the bottom of the gel.

175

176 Following electrophoresis, the gel was equilibrated in the transfer buffer (25mM
177 Tris, 192mM glycine and 20% (v/v) methanol at pH 8.3) for 10 min before
178 blotted for 2 hr at 250mA with voltage limit of 25 V onto a polyvinylidene
179 difluoride membrane. Membranes were blocked with 5% bovine serum albumin
180 in TBST buffer (100mM Tris-HCl, 150mM NaCl, 0.05% Tween 20 and 0.05%
181 SDS) overnight and incubated with primary antibody. For myosin heavy chain,
182 the membranes were incubated with 1:500 dilution of monoclonal anti-myosin
183 (skeletal, fast) (M4276, Sigma-Aldrich, USA) and monoclonal anti-myosin
184 (skeletal, slow) (M8421, Sigma-Aldrich, USA) antibodies in 3% BSA in TBST
185 buffer. Monoclonal anti-troponin-T antibody (T6277, Sigma-Aldrich, USA) was
186 used as the primary antibody for troponin-T. After that, the membranes were
187 washed with TBST buffer for three times and subsequently incubated in

188 1:10,000 dilution of secondary antibody (anti-mouse IgG whole molecule
189 conjugated with alkaline phosphatase) (A3562, Sigma-Aldrich, USA). The
190 membranes were then washed with TBST buffer for three times and detected
191 using AP detection kit (Bio-Rad, USA). Protein bands were visualized using Gel
192 DocTM XR+ System (Bio-Rad, USA) and quantified with Image LabTM software
193 (Bio-Rad, USA).

194

195 The difference in the band intensity of myosin heavy chain and actin amongst
196 the treatment groups were determined statistically using one-way analysis of
197 variance (ANOVA) at 95% confidence level. The data analysis was conducted
198 using SAS software (version 9.1, SAS Inst. Inc., U.S.A.). The data is presented
199 as means \pm standard error of means (S.E.M.).

200

201 **Liquid chromatography mass spectrometry**

202 Crude protein was extracted from each muscle sample. Briefly, 0.2 g of muscle
203 sample in powder form was mixed with 1ml of cold buffer containing 100mM
204 Tris, pH 8.3 and 10 μ l protease inhibitor (Calbiochem®). The samples were
205 mixed thoroughly with vortex for 30s and centrifuged at 4°C for 20min at
206 15,000 g. The supernatant was carefully collected and the concentration was
207 determined using the Bradford assay [22].

208

209 Each protein sample (100 μ g) was reduced with 50mM DTT at 60°C for 60min
210 and alkylated with 50mM iodoacetamide in the dark for 45 min at room
211 temperature. Then, proteins were diluted with 50mM ammonium bicarbonate
212 and digested with trypsin at 37°C overnight. The digestion process was

213 stopped by adding 0.5% formic acid. Digested peptides were desalted using
214 C18 ZipTip pipette tips (Millipore, Billerica, USA) according to the supplier's
215 instructions, and resuspended in 0.1% formic acid.

216

217 The purified digested peptides were separated with reverse phase liquid
218 chromatography using a Dionex Ultimate 3000 RSLCnano system (Thermo
219 Fisher Scientific) and analyzed by tandem mass spectrometry using Orbitrap
220 Fusion mass spectrometry (Thermo Fisher Scientific). Peptide samples (200
221 were separated on the EASY-Spray Column Acclaim PepMap™ C18 100A
222 (200µm particle size, 500µm id × 25cm; Thermo Fisher Scientific) by a gradient
223 from 5% to 40% of buffer B (0.1% formic acid in acetonitrile) at 300nL/min flow
224 over 91 min. The remaining peptides were eluted by a short gradient from 40%
225 to 95% buffer B in 2 min.

226

227 The eluting peptides were analyzed using tandem mass spectrometry using
228 Orbitrap Fusion mass spectrometry. Full scan spectra were collected using the
229 following parameters: scan range 310-1800 m/z, resolving power of 120,000,
230 AGC target of 4.0 e5 (400,000), and maximum injection time of 50 ms. The
231 method consisted of 3 s Top Speed Mode where precursors were selected for a
232 maximum 3 s cycle. Only precursors with an assigned monoisotopic m/z and a
233 charge state of 2 – 7 were further analyzed for MS2. All precursors were filtered
234 using a 20 second dynamic exclusion window and intensity threshold of 5000.
235 The MS2 spectra were analyzed using the following parameters: rapid scan rate
236 with a resolving power of 60,000, AGC target of 1.0e2 (100), 1.6 m/z isolation

237 window, and a maximum injection time of 250 ms. Precursors were fragmented
238 by CID and HCD at normalized collision energy of 30% and 28%.

239

240 The raw data obtained was analyzed using Thermo Scientific™ Proteome
241 Discoverer™ Software Version 2.1 (Thermo Fisher Scientific) with searching
242 database of goat (*Capra hircus*) and mammalian downloaded from UniProt. The
243 parameters for searching were set as follows: missed cleavage: 2; MS1
244 tolerance: 10ppm; MS2 tolerance: 0.6Da; variable modification: oxidation (M),
245 deamidation of asparagine (N) and glutamine (Q); and fixed modification:
246 carbamidomethyl (C). All peptides were validated using the percolator©
247 algorithm based on q-value less than 1% false discovery rate.

248

249 Quantitative analysis of the data was analyzed using Perseus version 1.6.0.2 to
250 identify the differentially expressed proteins in the muscle between the control
251 and lovastatin-treated groups. Pair-wise comparison between control and each
252 lovastatin-treated group was conducted using Student T-test. Gene ontology
253 enrichment analysis and functional annotation of the identified proteins were
254 performed using Database for Annotation, Visualization and Integrated
255 Discovery (DAVID) version 6.8 (<https://david.ncifcrf.gov>) [23]. In addition, the
256 cell and molecular functions and canonical pathways of these proteins were
257 identified using Ingenuity® Pathway Analysis (IPA®) (Qiagen, Germany).

258

259 **Results**

260 **Histology**

261 The histological examinations showed that skeletal muscle of animals
262 supplemented with lovastatin suffered from light to moderate damage (Figure
263 1). Mild haemorrhage was observed in the Medium treatment group while
264 skeletal muscle of the High treatment group showed relatively severe
265 degeneration as compared to other treatment groups. Descriptive data for each
266 group is shown in Table 2. The Kruskal-Wallis test showed a significant
267 difference among the four groups. It was observed that the muscle of the
268 Control group was normal, with no signs of any degeneration. The scores of
269 necrosis, interstitial space and vacuolization of the Low treatment group were
270 similar ($P>0.05$) to the Control group, except the score of degeneration
271 ($P<0.05$). When the Medium and High treatment groups compared with the
272 Control group, the scores of degeneration, necrosis, interstitial space and
273 vacuolization were significantly different ($P<0.05$). The scores of necrosis,
274 interstitial space and vacuolization, but not of degeneration of Low treatment
275 group, were significantly different ($P<0.05$) with Medium treatment group. When
276 comparing the Medium and High treatment groups, only the scores of necrosis
277 and degeneration were significantly different ($P<0.05$) between both groups.

278

279 **Fig 1. Histological analysis on longissimus thoracis et lumborum muscle**
280 **of goats supplemented with naturally produced lovastatin.**

281 Control, Low, Medium and High represent 0, 2, 4 and 6 mg lovastatin/kg BW,
282 respectively.

283 Mild haemorrhage was observed in the Medium treatment group. Skeletal
284 muscle of High treatment group showed relatively severe degeneration as
285 compared to other treatment groups.

286 **Table 2. Histology scores of *longissimus thoracis et lumborum* muscle of goats supplemented with naturally produced**
 287 **lovastatin.**

Parameters	Control			Low			Medium			High		
	Median	Min	Max	Median	Min	Max	Median	Min	Max	Median	Min	Max
Necrosis	0 ^a	0	0	0 ^a	0	0	1 ^b	0	2	3 ^c	1	4
Degeneration	0 ^a	0	0	0 ^b	0	1	0 ^b	0	2	2 ^c	0	3
Interstitial space	0 ^a	0	0	0 ^a	0	0	1 ^b	0	3	1 ^b	0	3
Vacuolation	0 ^a	0	0	0 ^a	0	0	1 ^b	0	2	1 ^b	0	3

288 Control, Low, Medium and High represent 0, 2, 4 and 6 mg lovastatin/kg BW, respectively.

289 Data was presented as the median, minimum and maximum of the score.

290 ^{abc} = Score within a row with different superscripts differ significantly at p<0.05.

291

292

293 **Expressions of myosin heavy chain and actin**

294 The difference in the immunoreactivities of myosin heavy chain and actin of
295 longissimus thoracis et lumborum muscle in the goats supplemented with
296 various lovastatin levels is presented in Table 3. There were significant
297 differences in the expression of myosin heavy chain between the treatment
298 groups, while the expression of actin was found to be unaffected by lovastatin
299 supplementation. The immunoreactivities of myosin heavy chain in the High
300 treatment group were significantly lower than the Control, Low and Medium
301 treatment groups. In contrast, the immunoreactivities of myosin heavy chain
302 were similar between the Control, Low and Medium treatment groups.

303

304

305 **Expressions of myosin heavy chain and actin**

306 The difference in the immunoreactivities of myosin heavy chain and actin of
307 longissimus thoracis et lumborum muscle in the goats supplemented with
308 various lovastatin levels is presented in Table 3. There were significant
309 differences in the expression of myosin heavy chain between the treatment
310 groups, while the expression of actin was found to be unaffected by lovastatin
311 supplementation. The immunoreactivities of myosin heavy chain in the High
312 treatment group were significantly lower than the Control, Low and Medium
313 treatment groups. In contrast, the immunoreactivities of myosin heavy chain
314 were similar between the Control, Low and Medium treatment groups.

315

316 **Table 3. Differences in immunoreactivities of myosin heavy chain and**
317 **actin in *longissimus thoracis et lumborum* muscle of goats supplemented**
318 **with naturally produced lovastatin.**

Protein	Control	Low	Medium	High
Myosin heavy chain	0.36±0.01 ^a	0.36±0.00 ^a	0.36±0.01 ^a	0.35±0.00 ^b
Actin	0.38±0.00 ^a	0.39±0.00 ^a	0.39±0.00 ^a	0.38±0.00 ^a

319 Control, Low, Medium and High represent 0, 2, 4 and 6 mg lovastatin/kg BW,
320 respectively.

321 ^{ab} Mean within a row with different superscripts differ significantly at p<0.05.

322

323 **Differentially expressed proteins**

324 The present study identified approximately 400 proteins in the
325 *longissimus thoracis et lumborum* muscle of goat. Comparisons between control
326 and lovastatin-treated groups demonstrated that lovastatin supplementation
327 induced complex modifications to the protein expression patterns in the
328 *longissimus thoracis et lumborum* muscle of the goat. When the Low treatment
329 and Control groups were compared, there were 25 proteins down-regulated and
330 five proteins up-regulated in the Low treatment group (Table 4). When the
331 Medium treatment and Control groups were compared, 21 proteins were
332 observed to be down-regulated and five proteins up-regulated (Table 5). When
333 the Control and High treatment groups were compared, 23 proteins were down-
334 regulated and one protein was up-regulated in the muscle tissue (Table 6).

335

336 **Table 4. Differentially expressed proteins in *longissimus thoracis et lumborum* muscle of goats supplemented with 2mg**
 337 **lovastatin/ kg body weight.**

UniProt Accession	Description	Species	Coverage	# Unique Peptides	# AAs ¹	MW ² [kDa]	calc. pI ³	Control	Low	-Log p-value	Difference ⁴
<i>Carbohydrate metabolism</i>											
P06733	Alpha-enolase	<i>Homo sapiens</i>	24.65	3	434	47.14	7.39	30.04	23.77	5.68	-6.27
P00883	Fructose-bisphosphate aldolase A	<i>Oryctolagus cuniculus</i>	59.34	5	364	39.32	8.09	34.17	27.00	5.36	-7.17
P05065	Fructose-bisphosphate aldolase A	<i>Rattus norvegicus</i>	50.55	1	364	39.33	8.09	34.18	31.30	4.28	-2.88
P52210	Fructose-bisphosphate aldolase B	<i>Ovis aries</i>	7.14	1	364	39.61	8.37	29.14	24.36	2.42	-4.77
P06744	Glucose-6-phosphate isomerase	<i>Homo sapiens</i>	24.19	2	558	63.11	8.32	30.04	25.54	3.16	-4.50
P04406	Glyceraldehyde-3-phosphate dehydrogenase	<i>Homo sapiens</i>	29.25	1	335	36.03	8.46	31.64	24.20	3.27	-7.44
P00355	Glyceraldehyde-3-phosphate dehydrogenase	<i>Sus scrofa</i>	66.07	4	333	35.81	8.35	34.22	31.64	1.74	-2.58
Q5E9B1	L-lactate dehydrogenase B chain	<i>Bos taurus</i>	32.93	9	334	36.70	6.44	32.22	27.15	3.12	-5.07

P36871	Phosphoglucomutase-1	<i>Homo sapiens</i>	48.40	2	562	61.41	6.76	30.09	23.34	3.22	-6.75
P00559	Phosphoglycerate kinase 1	<i>Equus caballus</i>	48.44	6	417	44.57	8.41	31.73	28.67	2.62	-3.06
P15259	Phosphoglycerate mutase 2	<i>Homo sapiens</i>	34.78	2	253	28.75	8.88	32.27	26.82	4.66	-5.45
P16290	Phosphoglycerate mutase 2	<i>Rattus norvegicus</i>	37.94	3	253	28.74	8.72	32.71	27.44	3.01	-5.27
Q2KJJ9	Fructose-1,6-bisphosphatase isozyme 2	<i>Bos taurus</i>	44.25	12	339	36.74	7.66	29.12	30.36	2.01	1.23
<hr/> <i>Creatine metabolism</i> <hr/>											
Q9XSC6	Creatine kinase M-type	<i>Bos taurus</i>	76.64	2	381	42.96	7.12	33.51	27.49	2.67	-6.02
P06732	Creatine kinase M-type	<i>Homo sapiens</i>	48.82	3	381	43.07	7.25	33.19	30.04	1.99	-3.15
P00563	Creatine kinase M-type	<i>Oryctolagus cuniculus</i>	63.52	3	381	43.09	7.12	33.16	27.08	5.20	-6.08
Q5XLD3	Creatine kinase M-type	<i>Sus scrofa</i>	71.13	3	381	43.03	7.09	31.37	23.24	2.11	-8.12
<hr/> <i>Other metabolic process</i> <hr/>											
P00571	Adenylate kinase isoenzyme 1	<i>Sus scrofa</i>	52.58	2	194	21.63	8.31	30.70	25.83	3.83	-4.87
P07450	Carbonic anhydrase 3	<i>Equus caballus</i>	13.08	4	260	29.49	7.84	29.37	26.44	2.01	-2.93
Q5S1S4	Carbonic anhydrase 3	<i>Sus scrofa</i>	20.00	2	260	29.39	7.85	30.25	27.78	1.99	-2.47
Q96DG6	Carboxymethylenebutenolidase homolog	<i>Homo sapiens</i>	13.06	3	245	28.03	7.18	28.36	26.25	1.89	-2.11
<hr/> <i>Cell growth and development process</i> <hr/>											

P19633	Calsequestrin-1	<i>Rattus norvegicus</i>	10.59	1	406	46.42	4.12	26.74	23.23	3.35	-3.50
Q13642	Four and a half LIM domains protein 1	<i>Homo sapiens</i>	30.96	3	323	36.24	8.97	30.84	26.57	3.34	-4.27
Q6ZMU5	Tripartite motif-containing protein 72	<i>Homo sapiens</i>	11.11	1	477	52.70	6.48	25.96	27.96	1.92	2.01
P62633	Cellular nucleic acid-binding protein	<i>Homo sapiens</i>	7.34	1	177	19.45	7.71	22.56	25.60	4.25	3.04
<i>Other proteins</i>											
P02191	Myoglobin	<i>Cervus elaphus</i>	77.27	2	154	17.04	7.83	34.10	30.54	2.38	-3.56
P04250	Myoglobin	<i>Lagostomus maximus</i>	9.74	1	154	17.00	7.74	31.15	27.07	2.33	-4.09
P49773	Histidine triad nucleotide-binding protein 1	<i>Homo sapiens</i>	30.16	2	126	13.79	6.95	28.24	25.91	2.51	-2.33
O54724	Polymerase I and transcript release factor	<i>Mus musculus</i>	14.80	5	392	43.93	5.52	25.28	27.20	1.84	1.92
P50397	Rab GDP dissociation inhibitor beta	<i>Bos taurus</i>	11.69	4	445	50.46	6.25	23.31	25.43	1.81	2.13

338 Control and Low represent 0 and 2 mg lovastatin/kg BW, respectively.

339 ¹ # AAs: number of amino acids

340 ² MW: molecular weight

341 ³ calc. pI: calculated isoelectric point

342 ⁴ Difference: Difference in the intensity between Control and Low treatment groups.

344 **Table 5. Differentially expressed proteins in *longissimus thoracis et lumborum* muscle of goats supplemented with 4mg**
 345 **lovastatin/ kg body weight.**

UniProt Accession	Description	Species	Coverage	# Unique Peptides	# AAs ¹	MW ² [kDa]	calc. pI ³	Control	Medium	-Log p-value	Difference ⁴
<i>Carbohydrate metabolism</i>											
P06733	Alpha-enolase	<i>Homo sapiens</i>	24.65	3	434	47.14	7.39	30.04	23.38	5.72	-6.66
P00883	Fructose-bisphosphate aldolase A	<i>Oryctolagus cuniculus</i>	59.34	5	364	39.32	8.09	34.17	28.21	3.79	-5.97
P05065	Fructose-bisphosphate aldolase A	<i>Rattus norvegicus</i>	50.55	1	364	39.33	8.09	34.18	29.39	5.10	-4.79
P06744	Glucose-6-phosphate isomerase	<i>Homo sapiens</i>	24.19	2	558	63.11	8.32	30.04	24.70	3.90	-5.34
P04406	Glyceraldehyde-3-phosphate dehydrogenase	<i>Homo sapiens</i>	29.25	1	335	36.03	8.46	31.64	26.87	3.12	-4.77
P00355	Glyceraldehyde-3-phosphate dehydrogenase	<i>Sus scrofa</i>	66.07	4	333	35.81	8.35	34.22	32.02	1.86	-2.21
Q5E9B1	L-lactate dehydrogenase B chain	<i>Bos taurus</i>	32.93	9	334	36.70	6.44	32.22	27.73	2.52	-4.48
P36871	Phosphoglucomutase-1	<i>Homo sapiens</i>	48.40	2	562	61.41	6.76	30.09	23.07	4.95	-7.02

P00559	Phosphoglycerate kinase 1	<i>Equus caballus</i>	48.44	6	417	44.57	8.41	31.73	29.82	1.67	-1.91
P15259	Phosphoglycerate mutase 2	<i>Homo sapiens</i>	34.78	2	253	28.75	8.88	32.27	26.16	5.72	-6.11
P16290	Phosphoglycerate mutase 2	<i>Rattus norvegicus</i>	37.94	3	253	28.74	8.72	32.71	27.96	2.69	-4.75
Q2KJJ9	Fructose-1,6-bisphosphatase isozyme 2	<i>Bos taurus</i>	44.25	12	339	36.74	7.66	29.12	30.71	2.70	1.59

Creatine metabolism

Q9XSC6	Creatine kinase M-type	<i>Bos taurus</i>	76.64	2	381	42.96	7.12	33.51	28.29	2.93	-5.23
P06732	Creatine kinase M-type	<i>Homo sapiens</i>	48.82	3	381	43.07	7.25	33.19	28.65	4.20	-4.55
P00563	Creatine kinase M-type	<i>Oryctolagus cuniculus</i>	63.52	3	381	43.09	7.12	33.16	28.82	2.94	-4.34
Q5XLD3	Creatine kinase M-type	<i>Sus scrofa</i>	71.13	3	381	43.03	7.09	31.37	23.85	1.98	-7.52

Other metabolic process

P00571	Adenylate kinase isoenzyme 1	<i>Sus scrofa</i>	52.58	2	194	21.63	8.31	30.70	25.39	3.49	-5.31
Q5S1S4	Carbonic anhydrase 3	<i>Sus scrofa</i>	20.00	2	260	29.39	7.85	30.25	27.78	1.73	-2.47
P48644	Retinal dehydrogenase 1	<i>Bos taurus</i>	16.37	6	501	54.77	6.65	26.73	28.77	3.01	2.03

Cell growth and development process

P19633	Calsequestrin-1	<i>Rattus norvegicus</i>	10.59	1	406	46.42	4.12	26.74	24.11	2.56	-2.63
Q13642	Four and a half LIM domains protein 1	<i>Homo sapiens</i>	30.96	3	323	36.24	8.97	30.84	26.21	3.97	-4.63
P62633	Cellular nucleic acid-binding	<i>Homo sapiens</i>	7.34	1	177	19.45	7.71	22.56	25.47	3.99	2.91

protein											
Q2UVX4	Complement C3	<i>Bos taurus</i>	4.21	4	1661	187.1	6.84	24.33	27.35	1.68	3.02
4											
<hr/> <i>Other proteins</i> <hr/>											
P49773	Histidine triad nucleotide-binding protein 1	<i>Homo sapiens</i>	30.16	2	126	13.79	6.95	28.24	26.18	2.04	-2.06
Q2KHU5	O-acetyl-ADP-ribose deacetylase	<i>Bos taurus</i>	27.38	6	325	35.55	9.32	28.98	27.17	2.49	-1.82
Q09666	Neuroblast differentiation-associated protein	<i>Homo sapiens</i>	4.21	5	5890	628.7	6.15	24.64	26.70	1.78	2.05
0											

346 Control and Medium represent 0 and 4 mg lovastatin/kg BW, respectively.

347 ¹ # AAs: number of amino acids

348 ² MW: molecular weight

349 ³ calc. pI: calculated isoelectric point

350 ⁴ Difference: Difference in the intensity between Control and Medium treatment groups.

352 **Table 6. Differentially expressed proteins in *longissimus thoracis et lumborum* muscle of goats supplemented with 6mg**
 353 **lovastatin/ kg body weight.**

UniProt Accession	Description	Species	Coverage	# Unique Peptides	# AAs ¹	MW ² [kDa]	calc. pI ³	Control	High	-Log p- value	Difference ⁴
<i>Carbohydrate metabolism</i>											
P00883	Fructose-bisphosphate aldolase A	<i>Oryctolagus cuniculus</i>	59.34	5	364	39.32	8.09	34.17	31.71	1.74	-2.46
P05065	Fructose-bisphosphate aldolase A	<i>Rattus norvegicus</i>	50.55	1	364	39.33	8.09	34.18	31.90	1.50	-2.28
P08059	Glucose-6-phosphate isomerase	<i>Sus scrofa</i>	28.49	2	558	63.09	7.99	30.02	26.84	1.53	-3.18
P13707	Glycerol-3-phosphate dehydrogenase [NAD(+)], cytoplasmic	<i>Mus musculus</i>	22.92	6	349	37.55	7.17	31.84	28.48	3.05	-3.36
A8BQB4	Glycogen debranching enzyme	<i>Equus caballus</i>	14.94	7	1533	174.5 6	6.70	28.77	25.02	1.56	-3.75
P19858	L-lactate dehydrogenase A chain	<i>Bos taurus</i>	73.19	3	332	36.57	8.00	33.89	28.79	3.57	-5.10
Q5E9B1	L-lactate dehydrogenase B chain	<i>Bos taurus</i>	32.93	9	334	36.70	6.44	32.22	27.79	2.18	-4.43

Q08DP0	Phosphoglucomutase-1	<i>Bos taurus</i>	67.44	12	562	61.55	6.81	31.52	29.40	2.02	-2.12
P36871	Phosphoglucomutase-1	<i>Homo sapiens</i>	48.40	2	562	61.41	6.76	30.09	24.80	2.74	-5.29
P00559	Phosphoglycerate kinase 1	<i>Equus caballus</i>	48.44	6	417	44.57	8.41	31.73	28.20	2.32	-3.53
Q7SIB7	Phosphoglycerate kinase 1	<i>Sus scrofa</i>	48.68	4	417	44.53	7.90	31.74	28.13	2.29	-3.60
P15259	Phosphoglycerate mutase 2	<i>Homo sapiens</i>	34.78	2	253	28.75	8.88	32.27	27.74	1.48	-4.53
P60174	Triosephosphate isomerase	<i>Homo sapiens</i>	53.15	12	286	30.77	5.92	32.47	30.44	1.75	-2.03
K0J107	Malate dehydrogenase, mitochondrial	<i>Felis catus</i>	34.32	8	338	35.49	8.68	27.48	25.16	1.48	-2.32
Q99798	Aconitate hydratase, mitochondrial	<i>Homo sapiens</i>	10.64	5	780	85.37	7.61	26.52	23.92	1.48	-2.60
<hr/> <i>Creatine metabolism</i> <hr/>											
Q9XSC6	Creatine kinase M-type	<i>Bos taurus</i>	76.64	2	381	42.96	7.12	33.51	31.90	1.50	-1.62
P06732	Creatine kinase M-type	<i>Homo sapiens</i>	48.82	3	381	43.07	7.25	33.19	30.69	2.02	-2.50
P00563	Creatine kinase M-type	<i>Oryctolagus cuniculus</i>	63.52	3	381	43.09	7.12	33.16	30.81	1.87	-2.35
<hr/> <i>Other metabolic process</i> <hr/>											
Q96DG6	Carboxymethylenebutenolidase homolog	<i>Homo sapiens</i>	13.06	3	245	28.03	7.18	28.36	23.90	3.60	-4.47
A4Z6H0	Adenylosuccinate synthetase	<i>Sus scrofa</i>	17.07	1	457	50.07	8.51	26.37	22.85	1.79	-3.53

isozyme 1

Other proteins

Q1KZF3	Beta A globin chain	<i>Capra hircus</i>	82.76	13	145	16.01	7.30	30.85	26.54	3.04	-4.30
I1X3V1	Galectin	<i>Capra hircus</i>	26.47	3	136	14.81	5.10	26.96	24.71	2.59	-2.25
Q99497	Protein DJ-1	<i>Homo sapiens</i>	43.39	7	189	19.88	6.79	29.87	27.44	1.71	-2.44
P50397	Rab GDP dissociation inhibitor	<i>Bos taurus</i>	11.69	4	445	50.46	6.25	23.31	26.66	2.68	3.35

beta

354 Control and High represent 0 and 6 mg lovastatin/kg BW, respectively.

355 ¹ # AAs: number of amino acids

356 ² MW: molecular weight

357 ³ calc. pI: calculated isoelectric point

358 ⁴ Difference: Difference in the intensity between Control and High treatment groups.

359

360

361 The differentially expressed proteins were grouped on the basis of their
362 functional role in the following categories: carbohydrate metabolism, creatine
363 metabolism, other metabolic process, cell growth and development process and
364 others. Most of the proteins affected were involved in carbohydrate metabolism,
365 in which fructose-bisphosphate aldolase A, glucose-6-phosphate isomerase, L-
366 lactate dehydrogenase B chain, phosphoglucomutase-1, phosphoglycerate
367 kinase 1, and phosphoglycerate mutase 2 were down-regulated in all lovastatin
368 treatment groups when compared to the Control group. The muscle of the Low
369 and Medium treatment groups showed a down-regulation in the alpha-enolase
370 and glyceraldehyde-3-phosphate dehydrogenase when compared to the
371 Control group. Fructose-bisphosphate aldolase B was down-regulated in the
372 Low treatment group only, while glycerol-3-phosphate dehydrogenase [NAD⁺],
373 glycogen debranching enzyme, L-lactate dehydrogenase A, malate
374 dehydrogenase, aconitate hydratase and triosephosphate isomerase were
375 down-regulated in the High treatment group only. Simultaneously, fructose-1,6-
376 bisphosphatase isozyme 2 was up-regulated in the Low and Medium treatment
377 groups when compared to the Control group.

378

379 The present findings also observed the down-regulation of creatine
380 kinase M type in all of the lovastatin treatment groups when compared to the
381 Control group. In addition, there were a number of proteins involved in the other
382 metabolic processes that were identified to be differentially expressed in the
383 lovastatin treatment groups. For example, adenylate kinase isoenzyme 1 and
384 carbonic anhydrase 3 were down-regulated in the Low and Medium treatment
385 groups, while carboxymethylenebutenolidase homolog was found to be down-

386 regulated in the Low and High treatment groups. Adenylosuccinate synthetase
387 isozyme 1 was down-regulated in the High treatment group only when
388 compared to the Control group. Retinal dehydrogenase 1 was found to be up-
389 regulated in the Medium treatment group when compared to Control group.

390

391 There were also proteins involved in cell growth and development
392 processes found to be differentially expressed in the present study. For instance,
393 calsequestrin-1 and four and a half LIM domains protein 1 (FHL1) were down-
394 regulated, while cellular nucleic acid-binding protein was up-regulated in the
395 Low and Medium treatment groups when compared to the Control group.
396 Tripartite motif-containing protein 72 was found to be up-regulated in the Low
397 treatment group as compared to the Control group. Complement C3 was up-
398 regulated in the Medium treatment group as compared to the Control group.

399

400 The expressions of a number of proteins involved in other processes
401 were also identified to be regulated in the present study. Myoglobin and
402 histidine triad nucleotide-binding protein 1 were down-regulated while
403 polymerase I and transcript factor, and Rab GDP dissociation inhibitor beta
404 were up-regulated in the Low treatment group when compared to the Control
405 group. In addition, the Medium treatment group showed that histidine triad
406 nucleotide-binding protein 1 and O-acetyl-ADP-ribose deacetylase were down-
407 regulated, while neuroblast differentiation-associated protein was up-regulated.
408 In the High treatment group, beta A globin chain, galectin and protein DJ-1 were
409 down-regulated while Rab GDP dissociation inhibitor beta was up-regulated.

410

411 The differentially expressed proteins were subjected to IPA® analysis.
412 These proteins were identified to be associated with several possible canonical
413 pathways, which including glycolysis I, gluconeogenesis I, glucose and glucose-
414 1-phosphate degradation, creatine-phosphate biosynthesis and pyruvate
415 fermentation to lactate. Generally, these proteins were involved in a network of
416 carbohydrate metabolism, energy production, and skeletal and muscular system
417 development and function.

418

419 **Discussion**

420 Statins are the most widely used lipid lowering agents which inhibit
421 HMG-CoA reductase in the cholesterol biosynthesis pathway. Nevertheless, the
422 use of statins is reported to have adverse effects such as muscular pain,
423 cramps and/or stiffness on skeletal muscles in humans [24]. We had previously
424 reported that lovastatin effectively decreased methane production in goats [18].
425 Given the potential for myopathies at higher than recommended therapeutic
426 doses the effects of naturally produced statins on the skeletal muscles of
427 ruminants was a primary interest of ours. Hence, the present study examined
428 the effects of naturally produced lovastatin on the histology and proteome
429 profile of the representative goat skeletal muscle longissimus thoracis et
430 lumborum.

431

432 **Histology**

433 Histological examination in the present study showed that
434 supplementation of lovastatin had light to moderate adverse effects on the

435 longissimus thoracis et lumborum muscle. The dose levels of the lovastatin
436 supplementation are positively correlated to the extent of cellular damage on
437 the skeletal muscle as reported previously [25]. Supplementation of 2mg
438 lovastatin/kg BW induced the a low but noticeable degeneration of the muscle
439 fiber in the goats. At higher dosages (4 and 6 mg/kg) naturally produced statin
440 resulted in the higher degree of necrosis and degeneration, as well as larger
441 interstitial space and vacuolization in the skeletal muscle.

442

443 **Expression of myosin heavy chain and actin**

444 Statin supplementation is reported to be involved in a large augmentation
445 of reactive oxygen species production in skeletal muscle which induce
446 mitochondrial impairments, reduce biogenesis mechanisms and result in
447 muscular pain or myopathy [26]. Production of reactive oxygen species in the
448 skeletal muscle may oxidize and degrade the myofibrillar proteins. Myosin
449 heavy chain is the protein most sensitive to oxidation among the myofibrillar
450 proteins [27]. Previous studies observed a decrease in the concentration of
451 myosin heavy chain following the exposure to oxidants [20, 28]. High oxidative
452 conditions cause cross-linking, polymerization and aggregate formation in
453 myosin heavy chain through the formation of disulfide bonds, bityrosine and
454 carbonyl derivatives [20]. In the present study, western blot analysis showed a
455 slight degradation of myosin heavy chain only in the High treatment group.
456 Although histological examination found that there was cellular damage in the
457 Medium treatment group, there was no degradation on the myosin heavy chain
458 detected. On the other hand, actin has been reported to be relatively stable
459 under oxidative conditions [20, 28]. This may be attributable to the

460 inaccessibility of oxidation sites, in which myofibrillar suspensions may be
461 masked by the interaction of actin and myosin chains [28]. The present study
462 also demonstrated that lovastatin supplementation had no effect on the actin of
463 skeletal muscle in goat.

464

465 **Differentially expressed proteins**

466 The present proteomics analysis demonstrated that supplementation of
467 lovastatin induced modifications on the expression of a number of proteins,
468 regardless the concentration of lovastatin. This data suggests that lovastatin
469 had an effect on a wide range of biological functions in the muscle. Lovastatin
470 supplementation had impaired the energy production system in the skeletal
471 muscle, particularly in the metabolism of carbohydrate and creatine. Similar
472 observations have been reported on the extensor digitorum longus muscle of
473 rats treated for 2-months of 10mg atorvastatin/kg BW and 20mg fluvastatin/kg
474 BW [29]. The impairment in the energy production system could play a major
475 role in the development of muscle damage, which is consistent with the adverse
476 effects observed on the longissimus thoracis et lumborum muscle through
477 histological examination.

478

479 **Carbohydrate metabolism**

480 The present study showed that lovastatin supplementation down-
481 regulated proteins involving in glycolysis, gluconeogenesis and fructose
482 metabolism. For examples, alpha-enolase, fructose-bisphosphate aldolase A,
483 fructose-bisphosphate aldolase B, glucose-6-phosphate isomerase,
484 glyceraldehyde-3-phosphate dehydrogenase, phosphoglycerate kinase 1,

485 phosphoglycerate mutase 2 and triosephosphate isomerase are glycolytic
486 enzymes which were down-regulated following lovastatin supplementation. In
487 addition, phosphoglucomutase-1 that catalyzing the bi-directional inter-
488 conversion of glucose-1-phosphate and glucose-6-phosphate, was also down-
489 regulated following lovastatin supplementation. Glucose-1-phosphate is a
490 substrate for synthesis of UDP-glucose used to synthesis a variety of cellular
491 constituents, while glucose-6-phosphate is the first intermediate in glycolysis.

492

493 Glycolysis is an oxygen independent pathway that converts 6-carbon
494 glucose into pyruvate. Through this metabolic process, high energy adenosine
495 triphosphate (ATP) molecules and reduced nicotinamide adenine dinucleotide
496 (NADH) are generated. Similar observations of down-regulation of glycolytic
497 enzymes in the skeletal muscle have also reported previously in rat and the
498 down-regulation of glycolytic enzymes is a symptom of energy production failure,
499 and can contribute to muscle damage [29]. In humans, hereditary muscle
500 glycogenoses are characterized by defective glycolytic enzymes and leads to
501 different degree of myopathy [30].

502

503 Interestingly, glycogen debranching enzyme, mitochondrial malate
504 dehydrogenase and mitochondrial aconitase hydratase were identified to be
505 down-regulated in the High treatment group only when compared to the Control
506 group. Glycogen debranching enzyme is an important regulatory enzyme in
507 cellular glucose utilization and energy homeostasis. This bi-functional enzyme
508 exhibiting both of oligotransferase (oligo-1,4 to 1,4-glucoantransferase, EC
509 2.4.1.25) and glucosidase (amylo-1,6-glucosidase, EC 3.2.1.33) activities in a

510 single polypeptide chain. Along with phosphorylase, this enzyme catalyzes the
511 complete degradation of glycogen and the release of glucose-1-phosphate and
512 glucose [31]. Down-regulation of this enzyme indicates the reduction of glucose
513 degraded from glycogen, and would subsequently affect the rate of glycolysis in
514 the skeletal muscle.

515

516 Both, mitochondrial malate dehydrogenase and aconitate hydratase are
517 integral components in the tricarboxylic acid (TCA) cycle which playing crucial
518 roles in energy production and biosynthesis. Malate dehydrogenase reversibly
519 catalyzes the oxidation of malate to oxaloacetate, which is crucial in
520 regenerating oxaloacetate that can be utilized in the TCA cycle and amino acid
521 production [32]. Meanwhile, aconitate hydratase catalyzes the inter-conversion
522 of citrate, isocitrate and cis-aconitate in the TCA cycle [33]. Mitochondrial
523 aconitate hydratase is also involved in iron metabolism and is very sensitive to
524 reactive oxygen species [34]. Large augmentation of reactive oxygen species is
525 produced in the skeletal muscle and is associated with the induction of
526 mitochondrial impairment [26]. The present findings indicate that a high level of
527 lovastatin supplementation (6mg/kg BW) results in the impairment of
528 mitochondrial function, which is in agreement with Päävä et al. [35] reporting
529 reduction of mitochondria volume in skeletal muscle following aggressive statin
530 treatment.

531

532 Meanwhile, fructose-1,6-bisphosphate isozyme 2 was up-regulated in the
533 Low and Medium treatment groups. This enzyme catalyzes the hydrolysis of
534 fructose-1,6-bisphosphate to fructose-6-phosphate in the gluconeogenesis [36].

535 In glycolysis, fructose-6-phosphate is converted to fructose-1,6-bisphosphate by
536 phosphofructokinase. This step is one of the rate-limiting steps in the glycolytic
537 pathway. Up-regulation of fructose-1,6-bisphosphate isozyme 2 and the
538 suppression of glycolysis prevent the breaking down of glucose, and
539 subsequently the reduction in ATP production.

540

541 **Creatine metabolism**

542 Generally, statin supplementation is associated with the higher
543 concentration of creatine kinase in the blood plasma. The present study
544 observed a down-regulation of creatine kinase following the lovastatin
545 supplementation. Similarly, decrease of creatine kinase in the skeletal muscle of
546 goat was also observed in rat [29]. Creatine kinase is an enzyme catalyzes the
547 conversion of creatine to phosphocreatine by utilizing ATP. This enzyme also
548 catalyzes the reverse reaction to produce phosphocreatine and ATP. In tissues
549 utilizing a large amount of ATP such as skeletal muscle, creatine kinase
550 /phosphocreatine system plays a complex and multi-faceted role in regulating
551 cellular energy homeostasis [37]. The ATP regeneration capacity of creatine
552 kinase is very high and considerably exceeds both cellular utilization and
553 replenishment through glycolysis and oxidative phosphorylation [37].
554 Interestingly, previous study showed that the transgenic mice lacking either the
555 cytoplasmic or mitochondrial creatine kinase may develop muscle atrophy [38].
556 Together with proteins involved in carbohydrate metabolism, down-regulation of
557 creatine kinase indicated an impairment to the energy production system, which
558 may develop statin myopathy.

559

560 **Other metabolic process**

561 Down-regulation of adenylate kinase isozyme 1, adenylosuccinate
562 synthetase isozyme 1 and carbonic anhydrase 3 may impair the energy
563 production in the skeletal muscle. Adenylate kinase isozyme 1 and
564 adenylosuccinate synthetase isozyme 1 play an important role in cellular
565 energy homeostasis, and more specifically in adenine nucleotide metabolism.
566 Adenylate kinase isozyme 1 catalyzes the reversible transfer of phosphate
567 between ATP and adenosine monophosphate (AMP), while adenylosuccinate
568 synthetase isozyme 1 interconverts inosine monophosphate (IMP) and AMP to
569 regulate nucleotide levels in the tissue, and which contributes to the regulation
570 of glycolysis. Meanwhile, the lack of carbonic anhydrase 3 is suggested to
571 impair mitochondrial ATP synthesis in the gastrocnemius muscle of rat [39].
572 Furthermore, carbonic anhydrase 3 is also shown to provide protection to the
573 cells against free radicals [40].

574

575 Retinal dehydrogenase 1, glycerol-3-phosphate dehydrogenase [NAD⁺],
576 L-lactate dehydrogenase A chain and L-lactate dehydrogenase B chain are
577 involved in redox cofactor metabolism which plays a central role in meeting
578 cellular redox requirements of proliferating mammalian cells. Retinal
579 dehydrogenase 1 converts retinaldehyde to retinoic acid, which directly
580 catalyzes the regeneration of NADH. Glycerol-3-phosphate dehydrogenase
581 catalyzes the reversible conversion of dihydroxyacetone phosphate to glycerol-
582 3-phosphate, which involves the redox reaction of NADH and NAD⁺. Meanwhile,
583 lactate dehydrogenase catalyzes the conversion of pyruvate into lactate.
584 Usually, a large amount of lactate is generated in proliferating cells to allow high

585 glycolytic flux to support the generation of ATP and biosynthetic precursors [41].
586 At the same time, generation of lactate also involves the conversion of NADH to
587 NAD⁺ by lactate dehydrogenase. NAD⁺ is crucial as it is directly used to oxidize
588 precursors of some nucleotides and amino acids, and also many intermediates
589 of NAD⁺-dependent pathway are important precursors for biosynthesis [42].
590 Reduction in these proteins may affect the NADP dependent pathways, then
591 blocking the ATP production pathways.

592

593 **Cell growth and development process**

594 Reduction in the expression of calsequestrin and FHL1, that are involved
595 in muscle development, was associated with the muscle damage. Calsequestrin
596 is a Ca²⁺-binding protein, which has been showed to be decreased in
597 dystrophic mouse skeletal muscle [43], while mutation in FHL1 gene is
598 associated with myopathy [44]. FHL1 is a multifunctional protein likely to be
599 involved in ion channel binding and muscle development. Furthermore,
600 transport proteins such as beta A globin chain, myoglobin and polymerase I and
601 transcript release factor were also down-regulated following lovastatin
602 supplementation. Polymerase I and transcript release factor is a protein
603 associated with processes of vesicular transport and cholesterol homeostasis
604 [45].

605

606 The present findings also identified proteins involved in the muscle tissue
607 development (such as complement C3, tripartite motif-containing proteins 72,
608 and cellular nucleic acid binding protein) which were up-regulated following
609 lovastatin supplementation. Complement C3 is shown to be activated in skeletal

610 muscle injury and plays a key role in the regeneration of muscle tissue [46, 47].
611 Tripartite motif-containing proteins are expressed in the skeletal muscle to
612 regulate muscle coordination, atrophy and repair. This protein plays an vital role
613 as a negative regulator of IGF-induced muscle differentiation [48]. Meanwhile,
614 cellular nucleic acid binding protein has been reported recently that its
615 modifications which are indicated to play a role in myotonic dystrophy type 2
616 disease might result in muscle atrophy through affecting myofiber membrane
617 function [49]. Together with Rab GDP dissociation inhibitor beta which involved
618 in the regulation of vesicle-mediated cellular transport [50], up-regulation of
619 these proteins in the present study indicated that the mechanism associated
620 with tissue regeneration or repair was activated in the muscle tissue.

621

622 **Other proteins**

623 In addition to the energy production system, proteins involved in other
624 cellular processes were also affected by lovastatin. Proteins such as galectins,
625 histidine triad nucleotide-binding protein 1 and Protein DJ-1, which are in
626 involved in the regulation of the apoptotic pathway, were also down-regulated
627 following lovastatin supplementation. Galectins have a diverse range of
628 biological functions including regulation of pre-mRNA splicing, cell adhesion,
629 cell growth, differentiation, apoptosis and cell cycle [51], while protein DJ-1
630 plays an important role in cell protection against oxidative stress and cell death
631 [52].

632

633 Taken together, the present study has shown that lovastatin
634 supplementation down-regulates proteins involved in the energy production

635 system (particularly the glycolytic pathway and creatine metabolism), regardless
636 of the concentration of lovastatin. Supplementation with a high concentration of
637 lovastatin (6mg/ kg BW) could further impair the TCA cycle. Moreover,
638 supplementation of lovastatin also activates tissue regeneration or repair in the
639 muscle tissue. Furthermore, changes in the expression of proteins involved in
640 apoptosis and oxidative damage suggests an accentuated sensitivity of statin-
641 treated muscle to oxidative stress. Oxidative stress can promote increased
642 proteolysis and depress protein synthesis, and trigger many conditions
643 associated with muscle wasting [53]. Such perturbation in energy metabolism
644 and ATP synthesis may have profound effects on protein synthesis and
645 contribute to metabolic stress, which could play a major role in the development
646 of myopathy.

647

648 **Conclusions**

649 Histology scores indicated increasing muscle damage to the longissimus
650 thoracis et lumborum muscle of goats supplemented with increasing dosages,
651 particularly at 6mg/kg BW, of naturally produced lovastatin. In addition, western
652 blot analysis indicated that the immunoreactivity of myosin heavy chain was
653 only degraded in the muscle of goats supplemented with 6mg lovastatin/kg BW.
654 Proteomics analysis revealed that lovastatin supplementation induced complex
655 modifications to the carbohydrate metabolism, energy production, and skeletal
656 and muscular system development of skeletal muscle of goats which may have
657 contributed to the observed skeletal muscle damage. Putting together results of
658 the above three analyses, it is clear that supplementation of naturally-produced

659 lovastatin at 6 mg/kg BW is too high, which can adversely affecting health and

660 wellbeing of the animals.

661

- 686 5. Elghandour MMY, Vázquez JC, Salem AZM, Kholif AE, Cipriano MM,
687 Camacho LM, et al. *In vitro* gas and methane production of two mixed
688 rations influenced by three different cultures of *Saccharomyces*
689 *cerevisiae*. J Appl Anim Res. 2017; 45:389-395.
- 690 6. Salem AZM, Kholif AE, Elghandour MMY, Buendía G, Mariezcurrena MD,
691 Hernandez SR, et al. Influence of oral administration of *Salix babylonica*
692 extract on milk production and composition in dairy cows. Ital J Anim Sci.
693 2014; 13(1):10-14.
- 694 7. Wildenauer FX, Blotevogel KH, Winter J. Effect of monensin and 2-
695 bromoethanesulfonic acid on fatty acid metabolism and methane
696 production from cattle manure. Appl Microbiol and Biotechnol. 1984;
697 19(2):125–130.
- 698 8. Martin SA. Manipulation of ruminal fermentation with organic acids: a
699 review. J Anim Sci. 1998; 76(12):3123-3132.
- 700 9. Dohme F, Machmüller A, Wasserfallen A, Kreuzer M. Ruminal
701 methanogenesis as influenced by individual fatty acids supplemented to
702 complete ruminant diets. Lett Appl Microbiol. 2001; 32(1):47-51.
- 703 10. Lee SY, Yang SH, Lee WS, Kim HS, Shin DE, Ha JK. Effect of 2-
704 bromoethanesulfonic acid on *in vitro* fermentation characteristics and
705 methanogen population. Asian- Australas J Anim Sci. 2009; 22(1):42-48.
- 706 11. Williams YJ, Popovski S, Rea SM, Skillman LC, Toovey AF, Northwood
707 KS, et al. A vaccine against rumen methanogens can alter the
708 composition of archaeal populations. Appl Environ Microbiol. 2009;
709 75(7):1860-1866.

- 710 12. Mohammed N, Ajisaka N, Lila ZA, Hara K, Mikuni K, Hara K, et al. Effect
711 of Japanese horseradish oil on methane production and ruminal
712 fermentation in vitro and in steers. J Anim Sci. 2004; 82(6):1839-1846.
- 713 13. Jahromi MF, Liang JB, Ho YW, Mohamad R, Goh YM, Shokryazdan P.
714 Lovastatin production by *Aspergillus terreus* using agro-biomass as
715 substrate in solid state fermentation. J Biomed Biotechnol. 2012.
716 doi:10.1155/2012/196264.
- 717 14. Alberts W, Chen J, Kuron G. Mevinolin: a highly potent competitive
718 inhibitor of hydroxymethylglutaryl- coenzyme A reductase and a
719 cholesterol-lowering agent. Proc Natl Acad Sci U S A. 1980; 77(7):3957-
720 3961.
- 721 15. Wolin MJ, Miller TL. Control of rumen methanogenesis by inhibiting the
722 growth and activity of methanogens with hydroxymethylglutaryl-CoA
723 inhibitors. Int Congr Ser. 2006; 1293:131-137.
- 724 16. Azlan PM, Jahromi MF, Ariff MO, Ebrahimi M, Candyrine SCL, Liang JB.
725 *Aspergillus terreus* treated rice straw suppresses methane production
726 and enhances feed digestibility in goats. Trop Anim Health Prod. 2018;
727 50(3)565-571.
- 728 17. Ramírez-Restrepo CA, O'Neill CJ, López-Villalobos N, Padmanabha J,
729 McSweeney C. Tropical cattle methane emissions: the role of natural
730 statins supplementation. Anim Prod Sci. 2014; 54:1294-1299.
- 731 18. Candyrine SCL, Mahadzir MF, Garba S, Jahromi MF, Ebrahimi M, A.A
732 Samsudin, et al. Effects of naturally-produced lovastatin on feed
733 digestibility, rumen fermentation, microbiota and methane emissions in

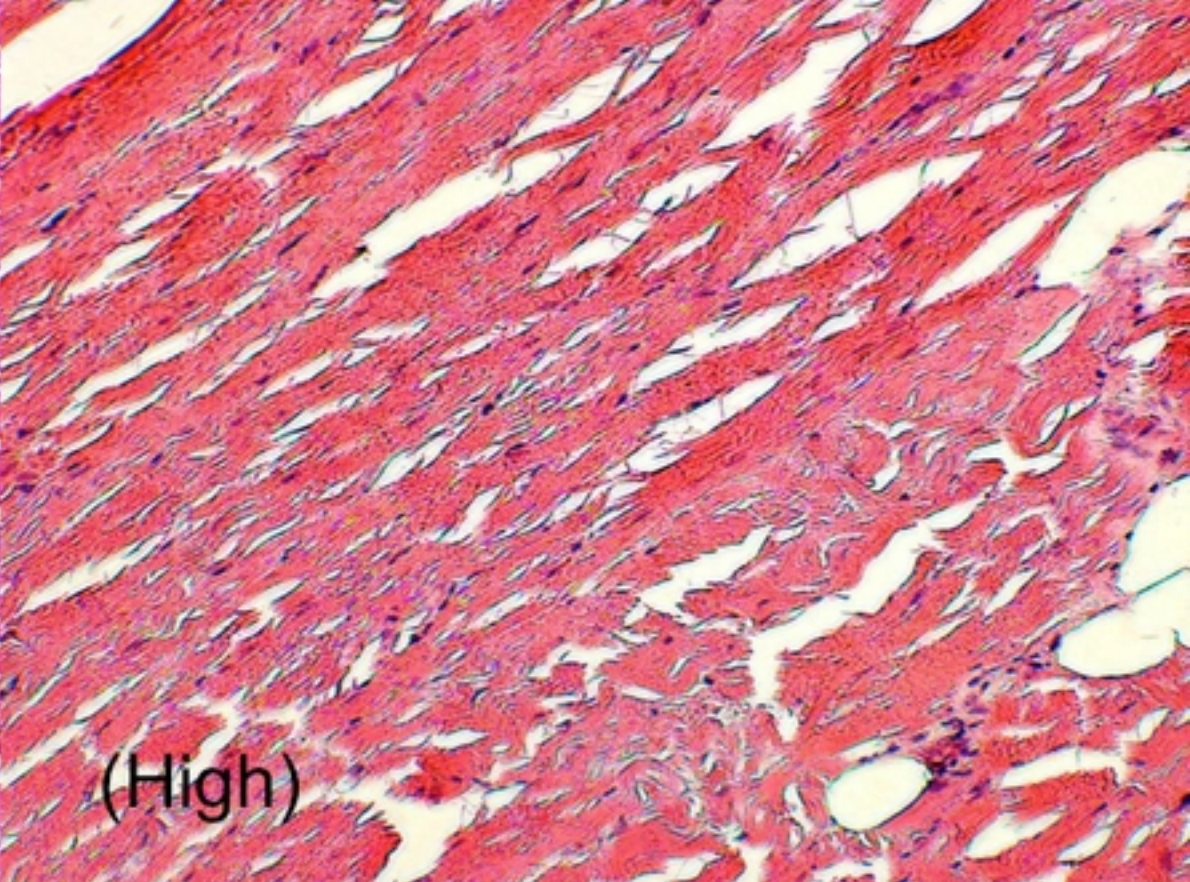
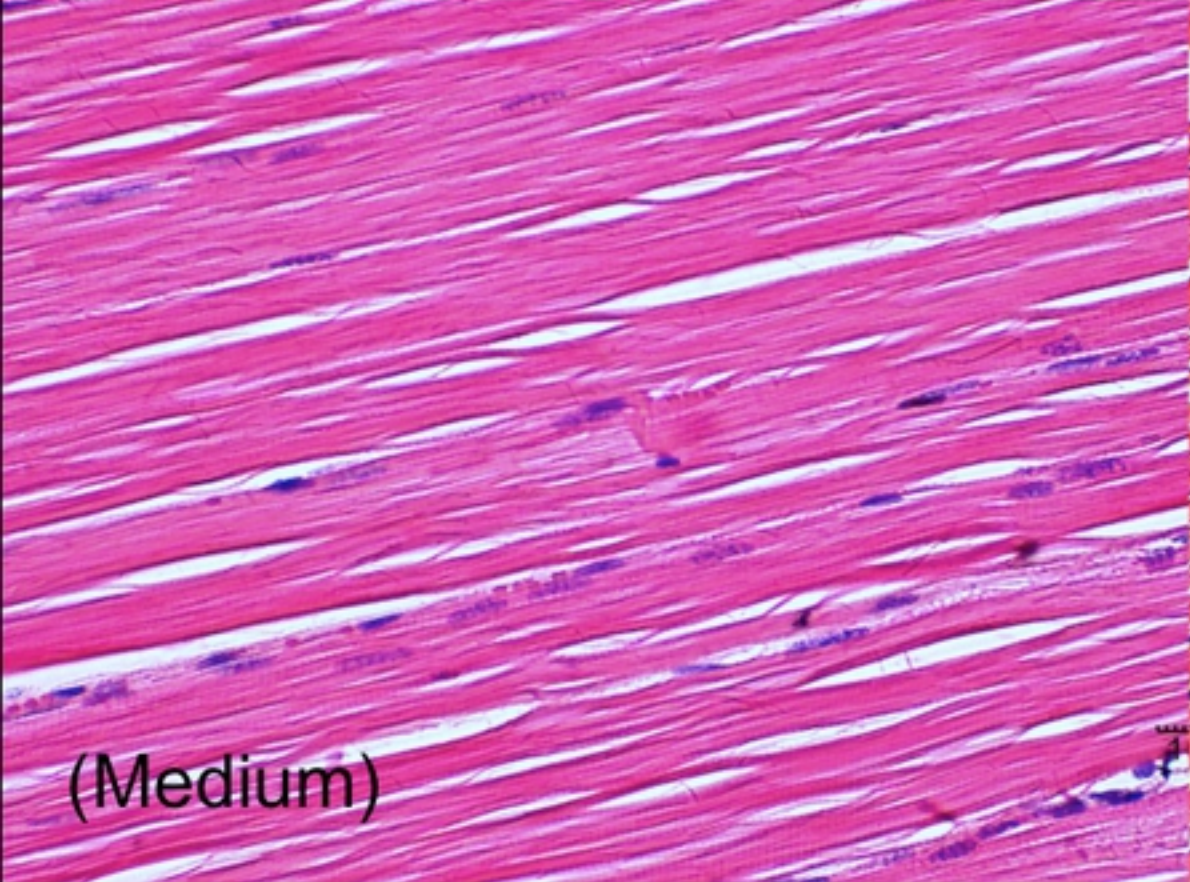
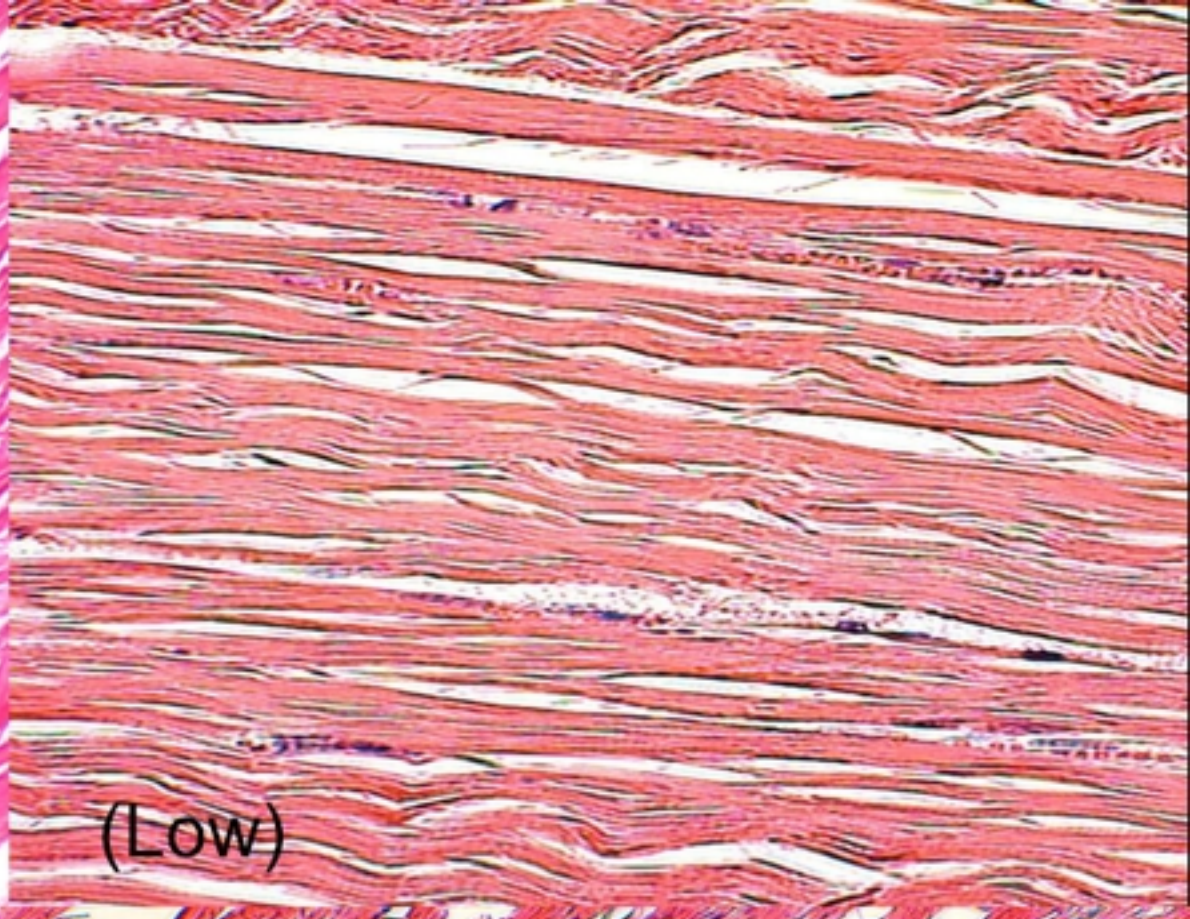
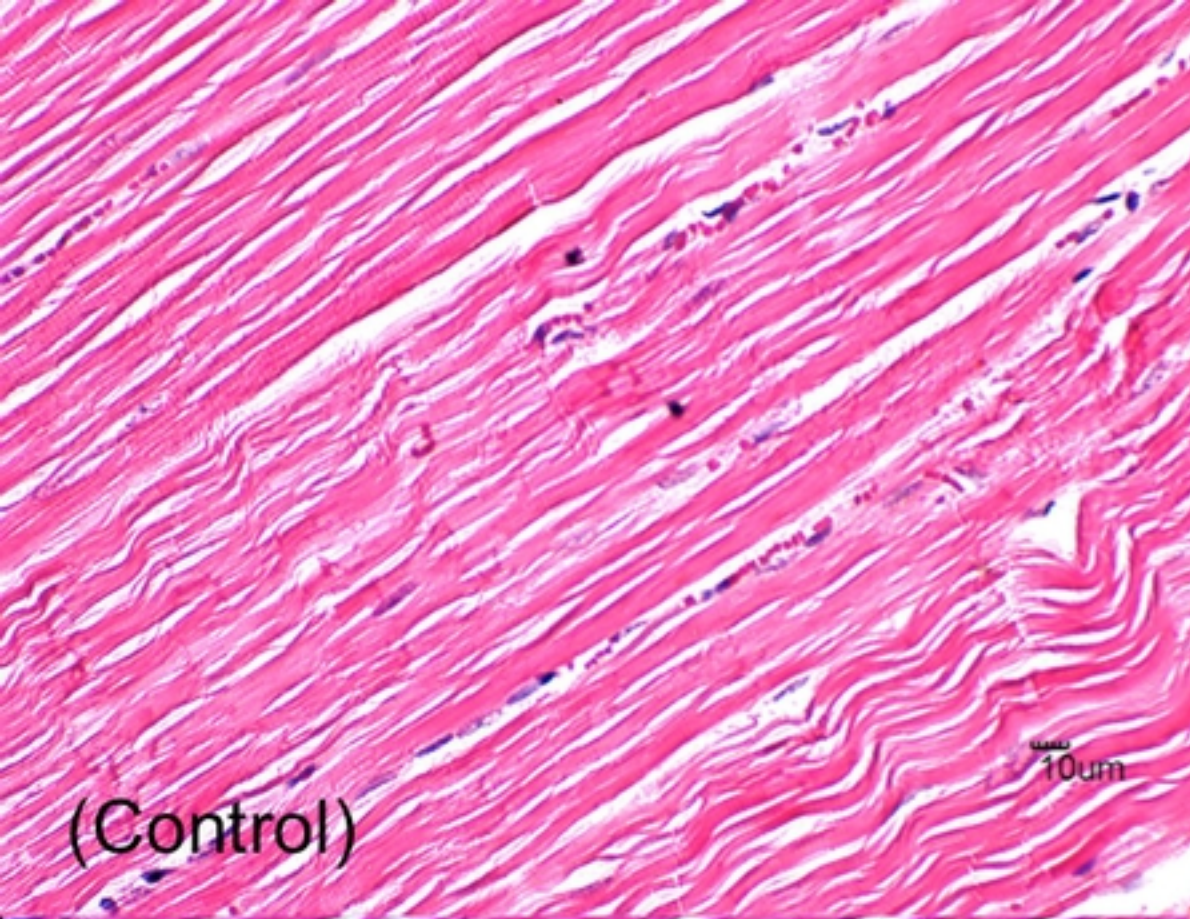
- 734 goats over a 12-week treatment period. PLOS ONE. 2018; 13(7):
735 e0199840. doi.org/10.1371/journal.pone.0199840.
- 736 19. Gall A, Treuting P, Elkon KB, Loo Y-M, Gale MJr, Barber GN, et al.
737 Autoimmunity initiates in non-hematopoietic cells and progresses via
738 lymphocytes in an interferon-dependent autoimmune disease. Immunity.
739 2012; 36(1):120-131.
- 740 20. Morzel M, Gatellier P, Sayd T, Renerre M, Laville E. Chemical oxidation
741 decreases proteolytic susceptibility of skeletal muscle myofibrillar
742 proteins. Meat Sci. 2006; 73(3):536-543.
- 743 21. Laemmli UK. Cleavage of structural proteins during the assembly of the
744 head of bacteriophage T4. Nature. 1970; 227(5259):680-685.
- 745 22. Bradford MM. A rapid and sensitive method for the quantitation of
746 microgram quantities of protein utilizing the principle of protein-dye
747 binding. Analyt Biochem. 1972; 72:248-254.
- 748 23. Huang DW, Lempicki RA, Sherman BT. Systematic and integrative
749 analysis of large gene lists using DAVID bioinformatics resources. Nat
750 Protoc. 2009; 4(1):44-57.
- 751 24. Bruckert E, Hayem G, Dejager S, Yau C, Begaud B. Mild to moderate
752 muscular symptoms with high-dosage statin therapy in hyperlipidemic
753 patients - The PRIMO study. Cardiovasc Drugs and Ther. 2005; 19:403-
754 414.
- 755 25. Norata GD, Tibolla G, Catapano AL. Statins and skeletal muscles
756 toxicity: from clinical trials to everyday. Pharmacol Res. 2014; 88:107-
757 113.

- 758 26. Bouitbir J, Charles A, Echaniz-laguna A, Kindo M, Daussin F, Auwerx J,
759 et al. Opposite effects of statins on mitochondria of cardiac and skeletal
760 muscles : a 'mitohormesis' mechanism involving reactive oxygen species
761 and PGC-1. *Eur Heart J.* 2012; 33:1397-1407.
- 762 27. Sun W, Cui C, Zhao M, Zhao Q, Yang B. Effects of composition and
763 oxidation of proteins on their solubility, aggregation and proteolytic
764 susceptibility during processing of Cantonese sausage. *Food Chem.*
765 2011; 124(1):336-341.
- 766 28. Xue M, Huang F, Huang M, Zhou G. Influence of oxidation on myofibrillar
767 proteins degradation from bovine via μ -calpain. *Food Chem.* 2012;
768 134(1):106-112.
- 769 29. Camerino GM, Pellegrino MA, Brocca L, Digennaro C, Camerino DC,
770 Pierno S, et al. Statin or fibrate chronic treatment modifies the proteomic
771 profile of rat skeletal muscle. *Biochem Pharmacol.* 2011; 81(8):1054-
772 1064.
- 773 30. DiMauro S, Lamperti C. Muscle glycogenoses. *Muscle Nerve.* 2001;
774 24(8):984-999.
- 775 31. Nakayama A, Yamamoto K, Tabata S. Identification of the catalytic
776 residues of bifunctional glycogen debranching enzyme. *J Biol Chem.*
777 2001; 276(31):28824-28828.
- 778 32. Gamberi T, Fiaschi T, Valocchia E, Modesti A, Mantuano P, Rolland J, et
779 al. Proteome analysis in dystrophic mdx mouse muscle reveals a drastic
780 alteration of key metabolic and contractile proteins after chronic exercise
781 and the potential modulation by anti-oxidant compounds. *J Proteomics.*
782 2018; 170:43-58.

- 783 33. Koen AL, Goodman M. Aconitate hydratase isozymes: subcellular location,
784 tissue distribution and possible subunit structure. *Biochim Biophys Acta*.
785 1969; 698-701.
- 786 34. Matasova LV, Popova TN. Aconitate hydratase of mammals under
787 oxidative stress. *Biochem (Mosc)*. 2008; 73(9):957-964.
- 788 35. Päivä H, Thelen KM, Coster RV, Smet J, Paepe BD, Mattila KM, et al.
789 High-dose statins and skeletal muscle metabolism in humans: a
790 randomized, controlled trial. *Clin Pharmacol Ther*. 2005; 78(1):60-68.
- 791 36. Marcus F, Gontero B, Harrsch PB, Rittenhouse J. Amino acid sequence
792 homology among fructose-1,6-bisphosphatases. *Biochem Biophys Res*
793 *Commun*. 1986; 135(2):374-381.
- 794 37. Wallimann T, Wyss M, Brdiczka D, Nicolay K, Eppenberger HM.
795 Intracellular compartmentation, structure and function of creatine kinase
796 isoenzymes in tissues with high and fluctuating energy demands: the
797 'phosphocreatine circuit' for cellular energy homeostasis. *Biochem J*.
798 1992; 281:21-40.
- 799 38. Momken I, Lechene P, Koulmann N, Fortin D, Mateo P, Doan BT, et al.
800 Impaired voluntary running capacity of creatine kinase-deficient mice. *J*
801 *Physiol* 2005; 565:951-964.
- 802 39. Liu M, Walter GA, Pathare NC, Forster RE, Vandenborne K. A
803 quantitative study of bioenergetics in skeletal muscle lacking carbonic
804 anhydrase III using ³¹P magnetic resonance spectroscopy. *Proc Natl*
805 *Acad Sci U S A*. 2007; 104(1):371-376.

- 806 40. Räsänen SR, Lehenkari P, Tasanen M, Rahkila P, Härkönen PL,
807 Väänänen HK. Carbonic anhydrase III protects cells from hydrogen
808 peroxide-induced apoptosis. *FASEB J.* 1999; 13:513-522.
- 809 41. Vander Heiden MG, Cantley LC, Thompson CB. Understanding the
810 Warburg effect: the metabolic requirements of cell proliferation. *Science.*
811 2009; 324(5930): 1029-1033.
- 812 42. Lunt SY, Vander Heiden MG. Aerobic glycolysis: meeting the metabolic
813 requirements of cell proliferation. *Annu Rev Cell Dev Biol.* 2011; 27:441-
814 464.
- 815 43. Doran P, Dowling P, Lohan J, McDonnell K, Poetsch S, Ohlendieck K.
816 Subproteomics analysis of Ca²⁺-binding proteins demonstrates
817 decreased calsequestrin expression in dystrophic mouse skeletal muscle.
818 *Eur J Biochem.* 2004; 271:3943-3952.
- 819 44. Windpassinger C, Schoser B, Straub V, Hochmeister S, Noor A,
820 Lohberger B, et al. An X-linked myopathy with postural muscle atrophy
821 and generalized hypertrophy, termed XMPMA, is caused by mutations in
822 FHL1. *Am J Hum Genet.* 2008; 82:88-99.
- 823 45. Cohen AW, Hnasko R, Schubert W, Lisanti MP. Role of caveolae and
824 caveolins in health and disease. *Physiol Rev.* 2004; 84:1341-1379.
- 825 46. Han R, Frett EM, Levy JR, Rader EP, Lueck JD, Bansal D, et al. Genetic
826 ablation of complement C3 attenuates muscle pathology in dysferlin-
827 deficient mice. *J Clin Investig.* 2010; 120(12):4366-4374.
- 828 47. Zhang C, Wang C, Li Y, Miwa T, Liu C, Cui W, et al. Complement C3a
829 signaling facilitates skeletal muscle regeneration by regulating monocyte
830 function and trafficking. *Nat Commun.* 2017; 8:2078.

- 831 48. Lee CS, Yi J, Jung S, Kim B, Lee N, Choo H, et al. TRIM72 negatively
832 regulates myogenesis via targeting insulin receptor substrate-1. *Cell*
833 *Death Differ.* 2010; 17:1254-1265.
- 834 49. Wei C, Stock L, Schneider-Gold C, Sommer C, Timchenko NA,
835 Timchenko L. Reduction of cellular nucleic acid binding protein encoded
836 by a myotonic dystrophy type 2 gene causes muscle atrophy. *Mol Cell*
837 *Biol.* 2018. doi:10.1128/MCB.00649-17.
- 838 50. Bachner D, Sedlacek Z, Korn B, Hameister H, Poustka A. Expression
839 patterns of two human genes coding for different rab GDP-dissociation
840 inhibitors (GDIs), extremely conserved proteins involved in cellular
841 transport. *Hum Mol Genet.* 1995; 4(4):701-708.
- 842 51. Kuwabara I, Sano H, Liu F-T. Functions of galectins in cell adhesion and
843 chemotaxis. *Methods Enzymol.* 2003; 363:532-552.
- 844 52. Clements CM, McNally RS, Conti BJ, Mak TW, Ting JP. DJ-1, a cancer
845 and Parkinson's disease-associated protein, stabilizes the antioxidant
846 transcriptional master regulator Nrf2. *Proc Natl Acad Sci U S A.* 2006;
847 103(41):15091-15096.
- 848 53. Powers SK, Smuder A, Judge A. Oxidative stress and disuse muscle
849 atrophy: cause or consequence? *Curr Opin Clin Nutr Metab Care.* 2012;
850 15(3):240-245.
- 851



Figure